Application of the Hilbert-Huang Transform to identification of changes in boundary conditions of a bridge using vibration data due to traffic

Arturo González[1,a] and Hussein Aied[1,b]

[1]University College Dublin; School of Civil, Structural and Environmental Engineering; Newstead, Belfield; Dublin 4; Ireland

[a]arturo.gonzalez@ucd.ie, [b]hussein.aied@ucdconnect.ie

Keywords: boundary conditions, bearings, non-linear dynamics, bridge.

Abstract. The translational restraints associated to pin and rocker bearings are typically idealized in the form of fixed and free conditions. However, elastomeric bearings need to be represented with springs to reasonably predict the time- and frequency-domain response of bridges under traffic-induced vibrations. Therefore, changes in the response of these bearings are common as a result of aging, deterioration, variation in loading levels and/or environmental changes. The latter makes difficult to discern if changes in the frequency content of the structural response to ambient vibration are due to changes in temperature, changes in normal operational loads or the occurrence of damage. In this paper, the bridge is idealized by a beam model supported on a hysteretic translational sprung support. The purpose is twofold: (a) to gather a better understanding of the variations of the bridge response with bearing performance; and (b) to be able to quickly identify an anomaly in the bearing. Empirical Mode Decomposition and the Hilbert-Huang Transform are employed to capture changes in the bearing stiffness from the bridge response.

Introduction

Elastomeric bridge bearings are the most commonly used type of seismic isolator and their main purpose is to increase the period of vibration of the bridge by inducing lateral flexibility. They are also used to allow bridge lateral movement due to temperature variation and earthquakes. Therefore, bearings can have a degree of compressibility in the vertical direction which is typically modeled with translational springs to attempt to resemble frequencies associated to vertical modes of vibration (in some cases, rotational springs are also used). There is experimental evidence that changes in the bridge frequencies can be attributed to changes in joints and elastomeric bearings [1]. Elastomeric bearings are nonlinear due to their inherent damping properties [2]. A number of mathematical hysteresis models of bearings to predict their response at different levels of stress are available in the literature [3-5]. The nonlinearity can be described by the restoring force and displacement behavior (hysteresis loop) which also describe the permanent (plastic) deformation in the bearings. A bilinear model can be used to accurately describe this bearing behavior at high deformations.

If the bearing is represented with a hysteresis loop spring model, the bridge frequencies may vary, i.e., there will be instantaneous frequencies that will depend on the load applied to the bearing and its stiffness. The level of change in frequency will be determined by the value of yield displacement defined in the constitutive model of the bearing. Lower yield displacement generally introduces more variations in bridge frequencies. While a Fast Fourier Transform (FFT) can be used to obtain the frequency of a linear model, this transform is not able to predict changes of frequency with time associated to non-linear models. In this regard, a number of methods have been employed to characterize the frequency content at each point in time such as wavelet analysis and the Hilbert transform. The wavelet analysis is effectively an adjustable window Fourier spectral analysis that is useful for linear data with a gradual change in frequency. For non-linear and non-stationary data, the

Hilbert transform use is limited as it can only define a 'monocomponent' signal (i.e., obtain only one frequency value for a single component) [6,7]. These limitations have been addressed by Huang et al. [8], who decompose the signal using Empirical Mode Decomposition (EMD) to obtain the Intrinsic Mode Functions (IMFs) and then use the Hilbert transform to obtain the instantaneous frequency of the signal. This methodology is called the Hilbert-Huang Transform (HHT) and it is one of the most popular methods for analysis of nonlinear and non-stationary data [8-10].

In the EMD process, the signal is decomposed into a number of IMFs using the 'sifting' procedure. The IMFs must satisfy two conditions: i) the number of extrema and the number of zero crossings must differ by no more than one, ii) the mean value of the envelope defined by the maxima and the minima at any given time must be zero. The sifting process to obtain the IMFs is as follows: i) identify the local maxima and minima, ii) find the mean of the upper and lower envelopes, iii) obtain h_1 the difference between the signal and the mean $h_1 = x(t) - m_1$. h_1 rarely satisfies the two conditions of IMFs and therefore h_1 is treated as the signal $h_1 - m_1 = h_{11}$ and the process is repeated k times to obtain the first IMF. Separating the first IMF c_1 (= h_{1k}) from the rest of data gives the residual $r_1 = x(t) - c_1$. The residual is used as the input signal to obtain the second IMF and the decomposition is repeated n times until the value of r_n becomes a monotonic component from which no more IMFs are extracted.

The second step of the HHT analysis is the Hilbert transform of the obtained IMFs [9]. The real part is taken as the j^{th} IMF signal $c_j(t)$, and the imaginary part is defined by the Hilbert transform (Eq. (1)).

$$y_i(t) = \frac{1}{\pi}\int_{-\infty}^{\infty} \frac{c_j(\tau)}{t-\tau} d\tau \tag{1}$$

The complex analytical signal given by Eq. (2) is formed.

$$z_i(t) = c_i(t) + jy_i(t) = a_i(t)e^{j\theta_i(t)} \tag{2}$$

where $a_i(t)$ is the amplitude at time t and $\theta_i(t)$ is the instantaneous phase. The instantaneous frequency can be obtained from Eq. (3).

$$\omega_i(t) = \frac{d\theta_i(t)}{dt} \tag{3}$$

Using the HHT analysis it is possible to characterize the instantaneous frequency of a nonlinear system such as a beam with non-linear sprung supports. System identification of the bearings under dynamic load has been investigated recently to accurately characterize the structural response [11]. Recent studies have also shown the applicability of the HHT in identification of damage in bridges [12] but its application to nonlinear bridge bearings has not received sufficient attention in the literature. HHT analysis can be helpful in the identification of stiffness reduction due to deterioration and aging which have been found to be a significant factor in bearing behavior [13] and shows that the effective stiffness of older bearings are more susceptible to cyclic load. This paper uses the HHT to identify changes in bearing stiffness based on the mid-span displacement of a discretized simply supported finite element beam with a pinned support at one end and a hysteresis (vertical translational) spring support at the other end.

Model to Simulate the Structural Response

A 1-D 10 m long Euler-Bernoulli beam is discretized into fifty 4-DOF elements. The beam is assumed homogenous with a modulus of elasticity of 3.5×10^{10} N/m^2 and density of 2400 kg/m^3. The beam section has an area of 7.2 m^2 and an inertia of 0.216 m^4. Viscous damping, typically low in bridges, is neglected in these simulations. A load of 10 tonnes moving at 20 m/s is applied to the

beam and displacement is calculated at midspan. The Wilson-θ method [14-16] is used here to integrate the equations of motion and to obtain the displacements, velocities and accelerations along the beam traversed by the load. Further details on this simulation model can be found in [17].

The beam is analysed with two types of right hand side (RHS) supports; roller and hysteretic vertical translational spring. The left hand support is assumed to always be pinned. If the data for elastomeric bearings is not available, AASHTO-LRFD Bridge Design Specification C14.7.5.3.3 allows for a linear fit of stress-strain relationship given by "K_v = E_vA/h_{rt}" [18,19] to define the stiffness of the elastomeric bearing (spring) which is employed here. In this relationship, K_v is the stiffness of the linear spring, and E_v is the elastic modulus of the spring given by $E_v = 6GS^2$, in which G is the shear modulus (that depends on the hardness and type of elastomeric bearing) assumed to be 0.69×10^6 N/m^2 and S is the shape factor assumed to be 12.3. A is the plan area of the elastomeric bearing (A = 0.1575 m^2 in this model) and h_{rt} (= 0.085 m) is the elastomeric bearing thickness (Fig. 1). Typical elastomeric bearing properties can be found in [20].

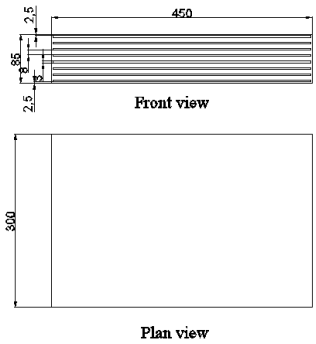

Fig. 1 – Elastomeric bearing (dimensions in mm)

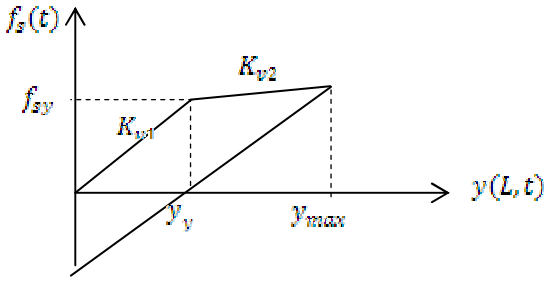

Fig. 2 – Hysteretic spring model

The constitutive model shown in Fig. 2 is used in this paper to model the bearing response. In this figure, the restoring force $f_s(t)$ is related to the displacement at the end of the beam $y(L,t)$, f_{sy} is the yield force corresponding to the yield displacement y_y, and y_{max} is the maximum displacement of the spring. A permanent displacement occurs once the yield displacement y_y is exceeded. The post-yield stiffness K_{v2} of the spring model is calculated based on Eq. (4) and the parameters defined above, which results into an stiffness value of 1.143752×10^9 N/m^2. The pre-yield stiffness $K_{v1}$is calculated based on a ratio of post-yield stiffness (K_{v2}) to pre-yield stiffness (K_{v1}) of 0.1 [21]. The yield displacement (y_y) and maximum displacement (y_{max}) of the spring are assumed to be 1×10^{-6} m and 1.05×10^{-4} m respectively.

Table 1 provides the frequencies obtained from an eigenvalue analysis of the beam model where the global stiffness matrix have been populared with the two RHS supports proposed here. For the hysteretic spring model, beam frequencies corresponding to the pre-yield stiffness (K_v=K_{v1}) and post-yield stiffness (K_v=K_{v2}) of the spring are given in the table. Differences between roller and spring support in the pre-yielding part of the curve are hardly noticeable for the lower frequencies.

Table 1 – Bridge Frequencies (Hz)

Bearing model/frequency	1st	2nd	3rd	4th
Roller	10.40	41.60	93.50	166.20
Spring with K_v=K_{v1} (pre-yield stiffness)	10.32	40.43	87.03	142.54
Spring with K_v=K_{v2} (post-yield stiffness)	9.72	30.78	58.91	111.09

The total displacement of the beam mid-span when traversed by a 10 tonne load at 20 m/s is separated into dynamic and static components and illustrated in Figs. 3(a) and 3(b) for the beam models with RHS roller and spring models respectively. When the load on the spring (reaction at the

RHS support) is small (i.e., far apart from the RHS support), its response remains in the pre-yielding part of the hysteretic model (Fig. 1(b)), and the beam has a similar mid-span displacement to that of the roller model due to its high K_{v1} stiffness. When the load approaches the RHS spring support, it comes a point when the restoring force exceeds the yield force, the post-yielding part of the spring model is entered and permanent deformation is caused. This permanent deformation can be visualized in the free vibration response of the beam in Fig. 3(b) (i.e., oscillations are not about zero). Figs. 3(c) and (d) show the Power Spectral Density (PSD) of the static and dynamic components in forced vibration in addition to the PSD of the record in free vibration. In Fig. 3(c), the 1st natural frequencies extracted from the forced and free vibration records (10.38Hz) are very close to eigenvalue analysis of the simulation (10.4 Hz). For such a relatively short simulation, small inaccuracies are unavoidable given that the level of discretization of the spectrum is determined by the duration of the record. The influence of the bearing post-yielding is not noticeable in Fig. 3(d) where a peak can be found near 10.32 Hz, which is the first natural frequency associated to the pre-yield stiffness.

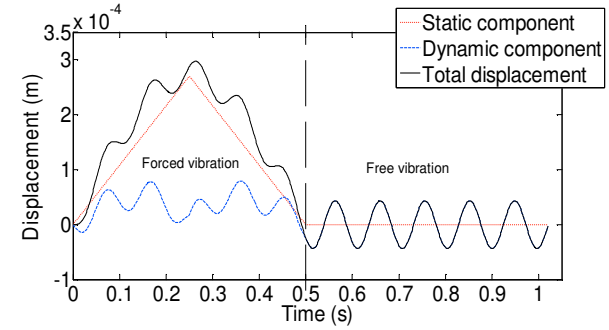

(a) Time domain response (RHS roller)

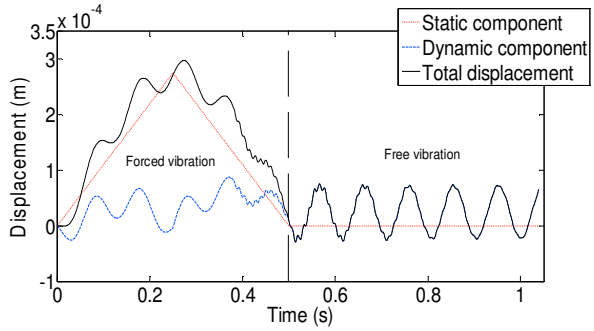

(b) Time domain response (RHS spring)

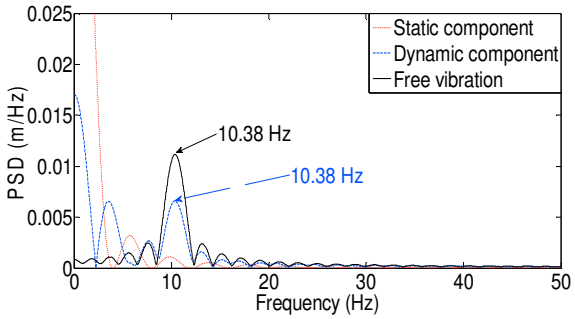

(c) PSD of beam response (RHS roller)

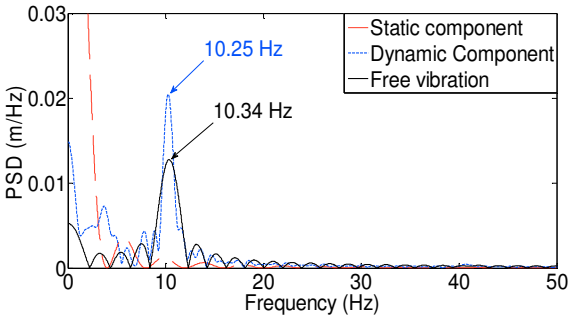

(d) PSD of beam response (RHS spring)

Fig. 3 – Components of the beam mid-span displacement for RHS roller and RHS spring supports

Beam Response Using Roller Model

EMD is applied separately to the forced and free vibration responses of the beam with RHS roller support in Figs. 4(a) and 4(b) respectively.

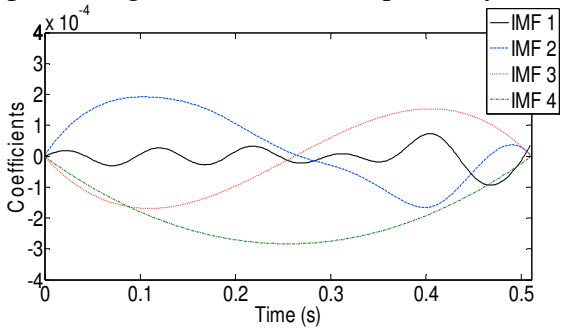

(a) forced vibration

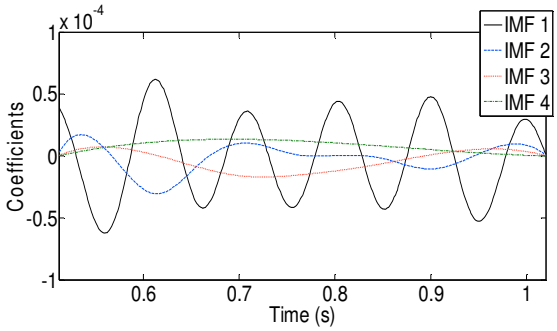

(b) free vibration

Fig. 4 – IMFs (RHS roller)

IMF 1 captures the 1st natural frequency of the system and this is illustrated by the PSDs shown in Fig. 5(a) and 5(b). IMF 1 contains dominant frequency components of 10.13 Hz and 10.28 Hz in forced and free vibration respectively. IMF 2 and IMF 3 have lower frequency components than IMF 1 as a result of the 'sifting' process employed in the EMD.

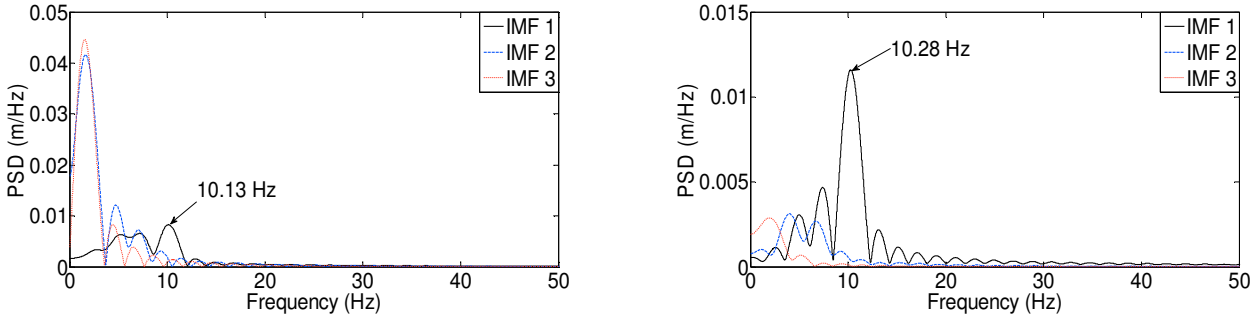

(a) forced vibration (b) free vibration

Fig. 5 – PSD of the IMFs of the beam response (roller support)

The time-frequency representation using the Mexican Hat Wavelet spectrum is compared to that using the HHT spectrum in Fig. 6. The wavelet spectrum is plotted using the Continuous Wavelet Transform (CWT) function which uses inner products to measure the similarity between the signal and an analysing function (Mexican Hat). Higher coefficients are brighter and indicate the dominant frequency at one point in time. In forced vibration, the most significant component of the response is static with low frequencies below 4 Hz (Fig. 6(a)). In free vibration, the wavelet reveals high coefficients between 9-11 Hz which is in the range of the 1st natural frequency of the beam. The Hilbert transform of the signal in free and forced vibration is plotted in Fig. 6(b) and 6(c) respectively. The frequency of IMF 1 is around 10 Hz (in agreement with Figs. 5(a) and 5(b)). Small variations of frequency with time are visible in forced vibration due to the influence of the static component of the response, but the IMF 1 is fairly consistent in identifying an almost constant instantaneous frequency (evidence of linearity).

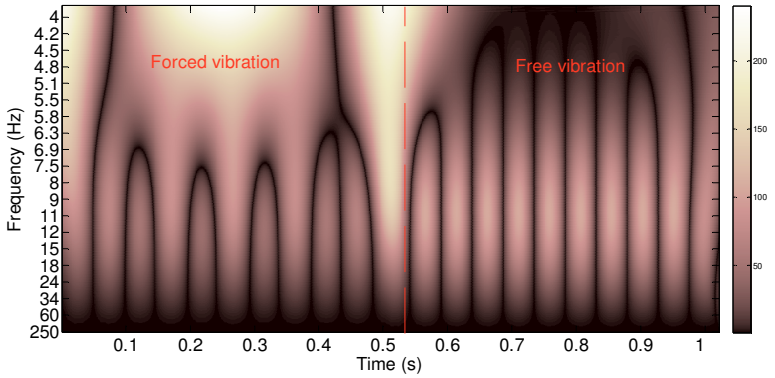

(a) CWT of total response

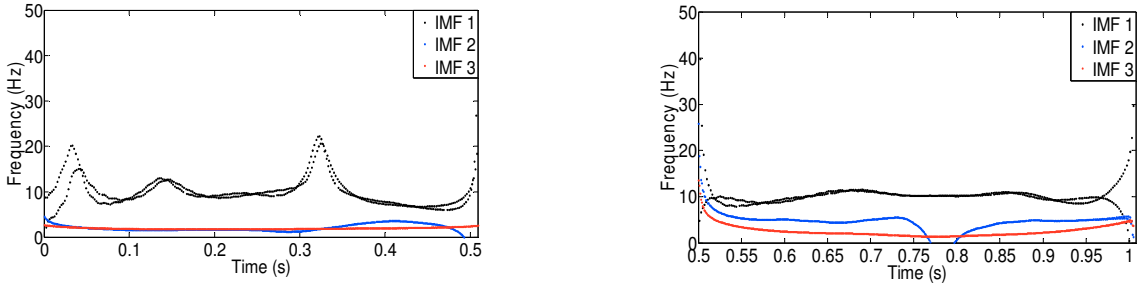

(b) HHT of forced vibration response (c) HHT of free vibration response

Fig. 6 – Frequency-time domain representations (RHS roller)

For a beam with a RHS roller support, the HHT provides a relatively smooth plot as a result of the linearity of the system. In this example, the IMF 1 is strongly linked to the first mode of vibration of

the beam. While the beam performs linearly and remains healthy, the HHT does not provide apparent advantages with respect to the PSD or CWT.

Beam Response Using Hysteretic Spring Model

In this case, a RHS spring support is included in the beam model and permanent deformation can be clearly distinguished in the free vibration displacement of Fig. 3(b) (i.e., oscillations are not about zero. The yield point has been exceeded during the load crossing and the RHS support has experienced some permanent deformation that is translated into a differential settlement between both supports, and as a result, a permanent settlement of the mid-span point where displacements are simulated). The IMFs of the total displacement in forced and free vibration are shown in Figs. 7(a) and 7(b) respectively.

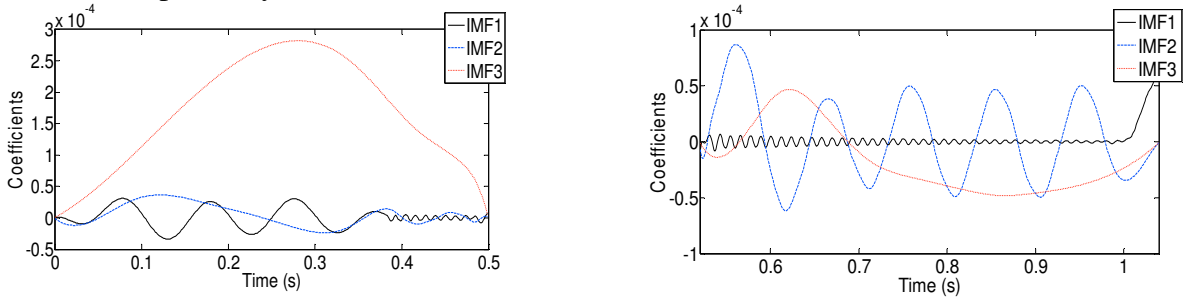

(a) forced vibration (b) free vibration

Fig. 7 – IMFs (RHS spring)

The PSDs of the IMFs in Fig. 7 are plotted in Fig. 8. IMF 1 is still associated to the 1st mode of vibration in forced vibration (Fig. 8(a)). However, unlike the case of the roller support, it is IMF 2 that captures most of the contribution of this mode to the free vibration response (Fig. 8(b)). Therefore, dominant frequencies are very close those corresponding to the pre-yielding stiffness (Table 1) given that the bearing experiences post-yielding only for a reduced period of time.

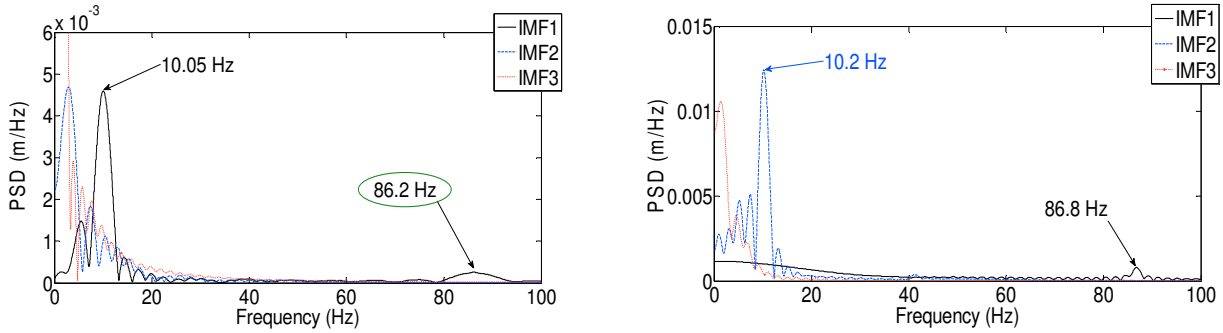

(a) forced vibration (b) free vibration

Fig. 8 – PSD of the IMFs of the beam response (RHS spring)

The CWT of the mid-span displacement is shown in Fig. 9(a). Higher coefficients illustrate the frequency corresponding to K_{v1}, which is in the range of 9.4-10.8 Hz, more clearly in free vibration. Previous research has succesfully applied CWT to the detection of localised losses of stiffness in the beam cross-section by identifying a local irregularity in the response to a moving load [14]. However, the latter is unable to capture losses of stiffness in sections of the bridge near a load entering or leaving a bridge due to edge effects. The area of influence of these edge effects is illustrated by the high coefficients near 0 and 0.5 seconds in Fig. 9(a). Here, the instant at which permanent bearing deformation occurs will be close to the supports and as a result, hindered to some extent from detection by wavelet analysis. The HHT of the mid-span displacement is shown in Fig. 9(b) and 9(c) in forced and free vibration respectively. Unlike the CWT, the HHT is able to reveal the change in stiffness of the bearing with a sudden increment in the instantaneous frequency of IMF 1 which occurs 0.38 seconds after the load entered the bridge (Fig. 9(b)). A wider scatter of

the instantaneous frequency remains between 0.38 and 0.51 seconds while the load keep increasing beyond the yield point. In free vibration (Fig. 9(c)), the instantaneous frequency for IMF 1 is widely scattered compared to Fig. 6(c), and it is the instantaneous frequency of IMF 2 the one fluctuating around 10 Hz reflecting the frequency associated to the pre-yield stiffness (which takes over once the load on the bearing decreases).

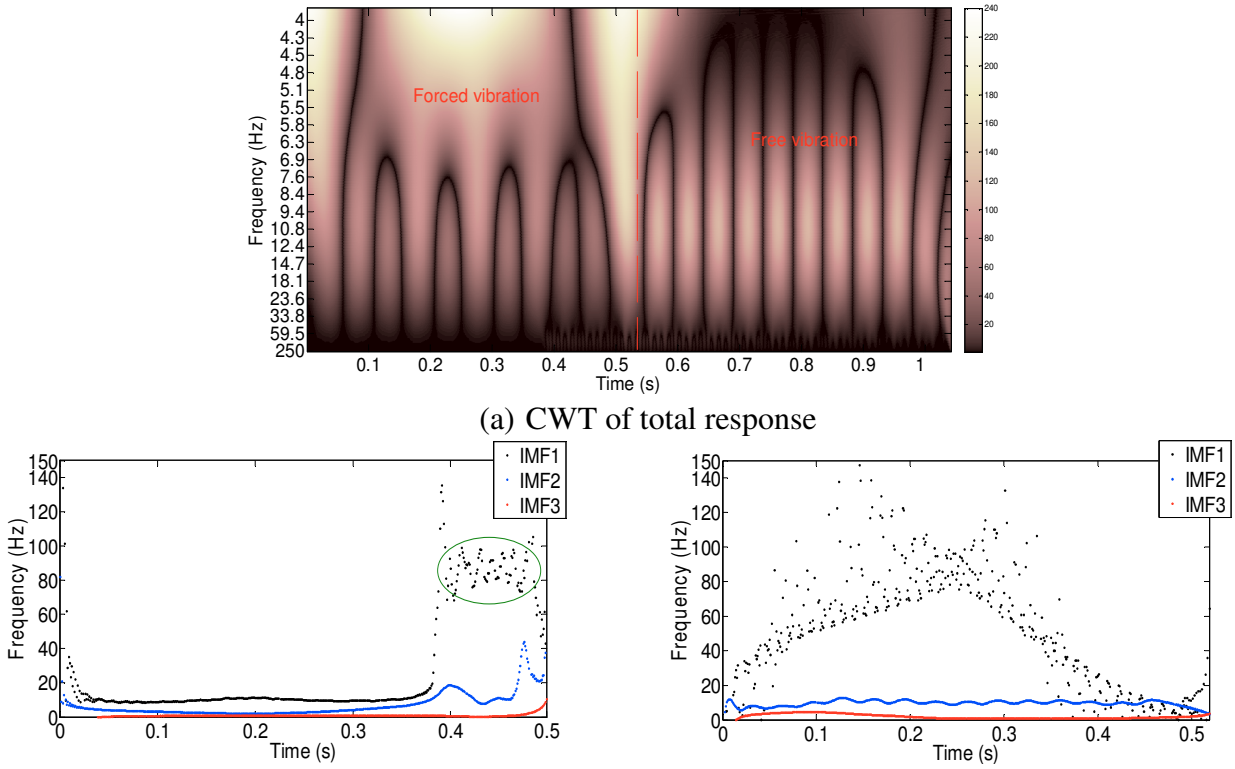

(a) CWT of total response

(b) HHT of forced vibration response

(c) HHT of free vibration response

Fig. 9 – Frequency-time domain representations (RHS spring)

Conclusions

Bearings are a major issue regarding bridge maintenance and durability. Periodic inspections of the bearings are labour expensive and time consuming, but they need to be undertaken to ensure that the bearings do not show signs of malfunctioning leading to distress of the bridge superstructure and if the latter was the case, to adopt preventive/remedial actions. This paper has proposed a method to establish the instant at which a bearing may cross the yield point leading to permanent deformation. This post-yield may last only a fraction before the load decreases and the bearing returns to perform with the original pre-yield stiffness value. In the latter, a PSD of a long record of measurements would be unable to appreciate a noticeable change in frequency that somehow could be related to this yielding. Therefore, there are obvious advantages in applying the HHT to the response of a beam when identifying changes of short duration in bearing performance that could denote damage. These changes will typically occur when the load is relatively near the support due to the larger reaction acting on the bearing. While the CWT experiences difficulties to detect irregularities near the supports due to edge effects, this paper has shown how the post-yielding of the bearing (or sudden change in stiffness) can be clearly identified by a sharp change in the instantaneous frequency of the HHT.

References

[1] P. Cornwell, C.R. Farrar, S.W. Doebling, H. Sohn, Environmental variability of modal properties, Experimental Techniques, 23 (2008) 45-48.

[2] M. Kikuchi, I.D. Aiken, An analytical hysteresis model for elastomeric seismic isolation bearings, Earthquake Engineering & Structural Dynamics, 26 (1997) 215-231.

[3] J.S. Hwang, J.D. Wu, T.C. Pan, G. Yang, A mathematical hysteretic model for elastomeric isolation bearings, Earthquake Engineering & Structural Dynamics, 31 (2002) 771-789.

[4] O. Hamzeh, J.L. Tassoulas, E.B. Becker, Analysis of Elastomeric Bridge Bearings, 1995.

[5] T.V. Pradeep, D.K. Paul, Force-deformation behavior of isolation bearings, J. of Bridge Engineering, 12 (2007) 527-529.

[6] M. Feldman, Non-linear system vibration analysis using Hilbert transform--II. Forced vibration analysis method 'Forcevib', Mechanical Systems and Signal Processing, 8 (1994) 309-318.

[7] M. Feldman, Non-linear system vibration analysis using Hilbert transform--I. Free vibration analysis method 'Freevib', Mechanical Systems and Signal Processing, 8 (1994) 119-127.

[8] N.E. Huang, Z. Shen, S.R. Long, M.C. Wu, H.H. Shih, Q. Zheng, N.C. Yen, C.C. Tung, H.H. Liu, The empirical mode decomposition and the Hilbert spectrum for nonlinear and non-stationary time series analysis, Proceedings of the Royal Society of London. Series A: Mathematical, Physical and Engineering Sciences, 454 (1998) 903-995.

[9] H. Huang, J. Pan, Speech pitch determination based on Hilbert-Huang transform, Signal Processing, 86 (2006) 792-803.

[10] G. Kerschen, A.F. Vakakis, Y.S. Lee, D.M. McFarland, L.A. Bergman, Toward a fundamental understanding of the Hilbert-Huang transform in nonlinear structural dynamics, J. of Vibration and Control, 14 (2008) 77-105.

[11] M.C. Huang, Y.P. Wang, J.R. Chang, C.C. Chien, Physical system identification of an isolated bridge using seismic response data, Structural Control and Health Monitoring,16 (2009) 241-265.

[12] A. Kunwar, R. Jha, M. Whelan, K. Janoyan, Damage detection in an experimental bridge model using Hilbert-Huang transform of transient vibrations, Structural Control and Health Monitoring, 20 (2013) 1-15.

[13] F. Casciati, L. Faravelli, Experimental investigation on the aging of the base isolator elastomeric component, Acta Mechanica, 223 (2012) 1633-1643.

[14] R.W. Clough, J. Penzien, Dynamics of Structures vol. 2, McGraw-Hill New York, 1993.

[15] R.E. Nickel, On the stability of approximation operators in problems of structural dynamics, International J. of Solids and Structures, 7 (1971) 301-319.

[16] R.R. Craig, Structural dynamics: An introduction to Computer Methods, Wiley New York, 1981.

[17] D. Hester, A. González, A wavelet-based damage detection algorithm based on bridge acceleration response to a vehicle, Mechanical Systems and Signal Processing, 28 (2012) 145-166.

[18] M.J. Whelan, K.D. Janoyan, Assessment of simplified linear dynamic analysis of a multispan skew bridge on steel-reinforced elastomeric bearings, J. of Bridge Engineering, 17 (2012) 151-160.

[19] AASHTO, LRFD Bridge Design Specifications, in 4th, ed. Washington, DC., 2007.

[20] S. Yamamoto, M. Kikuchi, M. Ueda, I.D. Aiken, Analytical modelling of elastomeric isolation bearings under severe axial load and shear deformations, in Proceedings of the 14th World Conference on Earthquake Engineering, Beijing, China, 2008.

[21] S. Muthukumar, A contact element approach with hysteresis damping for the analysis and design of pounding in bridges, PhD Thesis, 2003.